

Modeling Supercritical Systems With Tough2: The *EOS1sc* Equation of State Module and a Basin and Range Example

Tom H. Brikowski
Geosciences Dept., University of Texas at Dallas
Richardson, TX 75083 USA
email: brikowi@utdallas.edu

Abstract

A supercritical fluid equation of state module (*EOS1sc*) has been developed for use with the *TOUGH2* geothermal reservoir simulator. Supercritical fluid conditions ($T > 374^\circ\text{C}$) have been observed at depth in magmatic geothermal systems and are important in the deep heating zones of extensional geothermal systems as well. As interest in the sustainability of mature geothermal fields increases, and as exploration for high temperature resources becomes more attractive, the ability to model an entire field from ground surface to supercritical regions will become crucial. Tests using the *EOS1sc* module successfully reproduce sub-critical sample problem results of EOS1 (e.g. RVF, RFP). Supercritical validation suites are currently lacking, but preliminary models reasonably extend sub-critical model results to supercritical conditions. For example, generic models of extensional settings using *EOS1sc* with supercritical temperatures at depth better-simulate observed temperature depth profiles (e.g. Dixie Valley, NV) than EOS1-based models.

1 Introduction

Supercritical fluid conditions ($T > 374^\circ\text{C}$, Fig. 1) have been observed at depth in magmatic geothermal systems (Kakkonda, Japan; Ikeuchi *et al.*, 1998) and are implied in the deeper portions of extensional geothermal systems as well (Basin and Range, Nevada, USA; Wisian, 2000). As interest in the sustainability of mature geothermal fields increases, and as exploration for high temperature resources becomes more attractive (e.g. Iceland, Fridleifsson and Albertsson, 2000), the ability to model an entire field from ground surface to supercritical regions will become crucial. There are currently few options in selecting a supercritical geothermal reservoir modeling computer program. The most commonly-applied programs, *TOUGH2* (Pruess *et al.*, 1999) and *TETRAD* (Vinsome, 1990), are currently limited to sub-critical conditions (white area, Fig. 1). The most readily-available supercritical program (*HYDROTHERM*, Hayba and Ingebritsen, 1994) lacks some of the computational and gridding flexibility of *TOUGH2*. Given this situation, a super-critical equation-of-state (EOS) module for *TOUGH2* would be an attractive option; this paper introduces such a module, and demonstrates its current applicability.

2 Approach

Since no one of the codes listed above is capable of modeling supercritical conditions with the desired level of thermodynamic detail, as well as modeling dissolved species transport and water-rock interaction, some modification of the codes will be required. The apparent optimal choice for this hybrid is *TOUGH2*, modified to include first a supercritical equation of state (*H2092*), and later the oxygen-isotope alteration routines from *MARIAH*. The subject of this

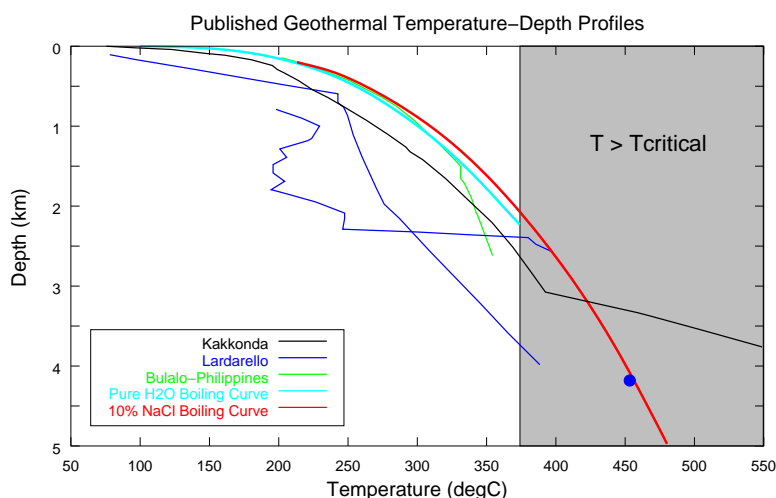


Figure 1: Pressure-depth profiles for deep geothermal systems, after Muraoka *et al.* (2000). Shaded area shows region of supercritical temperatures.

paper are the results of the first coding phase of the project, in which *H2092* will be adapted as an EOS module, to serve as a plug-in conversion to enable supercritical modeling. The supercritical equation of state module has been designated as “*EOS1sc*”, and its structure largely imitates that of the original EOS1 module available with *TOUGH2* (Pruess *et al.*, 1999). The implementation of *EOS1sc* extends the range of *TOUGH2* considerably, currently giving it an applicable range of $0 < T \leq 1000^\circ\text{C}$ and $0 < P \leq 1000$ MPa (Fig. 2)

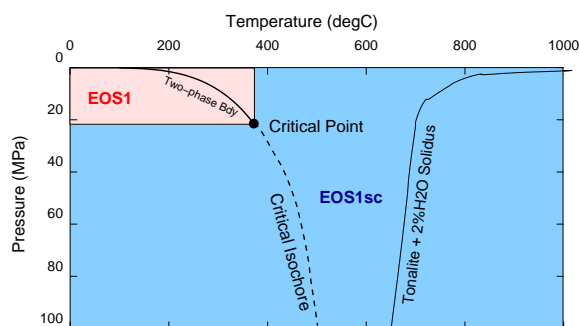


Figure 2: P-T Validity Range of EOS1 (pink shaded area, Pruess *et al.*, 1999) and *EOS1sc* (blue area). Liquid-vapor solidus of hydrous tonalite magma with 2 wt% H_2O shown to indicate typical magmatic conditions (Whitney, 1975). Dashed line shows approximate location of critical isochore (line of density equal to density at the critical point).

2.1 *H2092*

The numerical equation of state used in this modification, *H2092*, has been used in a number of previous supercritical applications (Norton and Hulen, 2000; Brikowski and Norton, 1989). It treats very accurately fluid properties and their extrema at the critical point (e.g. isobaric heat capacity theoretically reaches $+\infty$). These extrema have a profound effect on fluid dynamics, and accurate treatment of such properties is required for accurate reservoir models that include the critical region. *H2092* uses a Taylor series approximation for Helmholtz free

energy outside the critical region, from which most of the remaining fluid thermodynamic properties can be obtained via numerical differentiation (pg. 580, Johnson and Norton, 1991). In the vicinity of the critical point, the non-classical Levelt-Sengers equation for thermodynamic potential is used, which can be treated similarly to obtain fluid properties. Given input T-P or T- ρ , *H2092* computes a total of eighteen fluid thermodynamic properties and ratios. The Taylor series are based on physical considerations of the internal chemistry of the fluid, and as such can be far more accurate than strictly mathematical interpolations of these properties (e.g. International Formulation Committee, 1967). For systems containing critical-point conditions this accuracy is fundamentally important, but it comes at a steep computational cost, since the Taylor series require calculation of many more terms at each P-T point. The *H2092* code is freely available as a part of the SUPCRT aqueous geochemical modeling package (Johnson *et al.*, 1992).

2.2 Challenges

A number of conceptual and numerical challenges in this approach were predictable, and were encountered. Most problematic is the termination of the two-phase boundary at the critical point. All of the reservoir simulators listed above utilize phase mass-balances which are computed at every point in the system. Both steam and liquid “disappear” above the critical point, and become an indistinguishable supercritical fluid. At and above the critical point, this requires an artificial iso-enthalpic “reaction” (e.g. Hayba and Ingebritsen, 1994, p. 8) to convert steam or liquid into fluid. *HYDROTHERM* handles this problem by declaring 50% saturation with identical steam and liquid properties in supercritical regions. Since *TOUGH2* utilizes steam saturation as a primary (dependent) variable along the two-phase boundary, this approach was not an option. Instead an artificial extension to the two-phase boundary was implemented, across which a thermodynamically-neutral reaction of liquid and steam was allowed. Although many orientations for this extension are possible, extending it along the critical isochore (line of density equal to that at the critical point, dashed line, Fig. 2) was conceptually the simplest.

A more difficult problem is implied phase transitions (a super-critical cell with sub-critical neighbor). These lead to “subtle and complicated difficulties” (e.g. Pruess *et al.*, 1999, Appendix D) or (e.g. Hayba and Ingebritsen, 1994, p. 8) in computing accurate phase mass balances, and care must be taken to treat interfacial fluxes properly. Variable switching in *TOUGH2* to pressure-saturation along the two-phase boundary becomes somewhat problematic at the critical point. Finally, a problem that will never be completely eliminated is difficult convergence near the critical point. The incorporation of *H2092* is specifically intended to treat extrema in fluid properties accurately, based on the proposition that these extrema are the fundamental controls on fluid circulation and heat transport in deep systems. As a result spatial gradients in fluid properties are larger than with alternative equations of state described above. This leads to increased residuals (errors) in mass and energy balance equations, and increased difficulty in finding convergent solutions for problems with coarse grid and high advective flow rates. Unsmoothed initial conditions can also be problematic

3 Results

Tests of *EOS1sc* have been made in two categories. The first are sub-critical models run to confirm that existing capabilities of *TOUGH2* have not been degraded by the application of *EOS1sc*. The second explore the supercritical performance of *EOS1sc*, and are more limited,

since successful supercritical runs have only recently been achieved.

3.1 Sub-Critical Tests

For general familiarity, the two sample problems distributed with *TOUGH2* that invoke the EOS1 module were run for comparison. These are RFP, the “geothermal five-spot injection/production” problem (sec. 9.4, Pruess *et al.*, 1999), and RVF, the “heat sweep in a vertical fracture” problem. Both runs produce results that are graphically indistinguishable from the EOS1 results (Figs. 3 and 4. In detail, results differ by less than 0.01%, running in double-precision (REAL*8). As expected, a significant difference in run-times is apparent (Fig. 5), with the *EOS1sc* runs requiring 5 to 50 times longer on an SGI O2 R10000 workstation. Since memory usage is small, and disk access minimal in these test problems, similar time differences should be experienced on most computing platforms. Recall that EOS1 has been optimized for speed in sub-critical settings, while *EOS1sc* has been constructed for maximum accuracy in the near-critical region. Users wishing to apply *EOS1sc* should be thoroughly committed to thermodynamic accuracy versus computational speed.

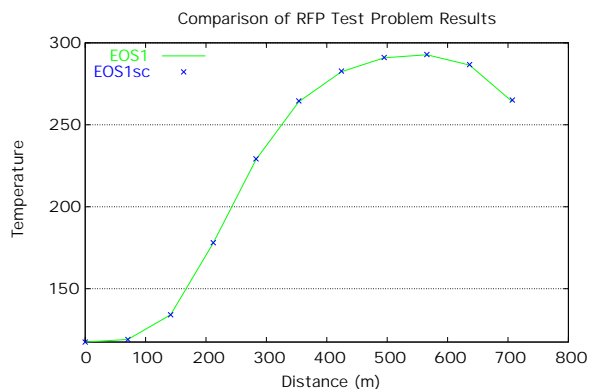


Figure 3: RFP (geothermal 5-spot well) test results for EOS1 (line) and *EOS1sc* (points) in *TOUGH2*. See Pruess *et al.* (sec. 9.4, 1999) for details of problem specification.

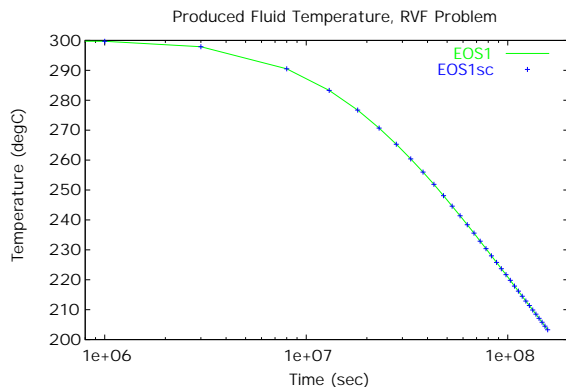


Figure 4: RVF (vertical fracture heat-sweep) test results using EOS1 (line) and *EOS1sc* (points) in *TOUGH2*. See Pruess *et al.* (sec. 9.3, 1999) for details of problem specification.

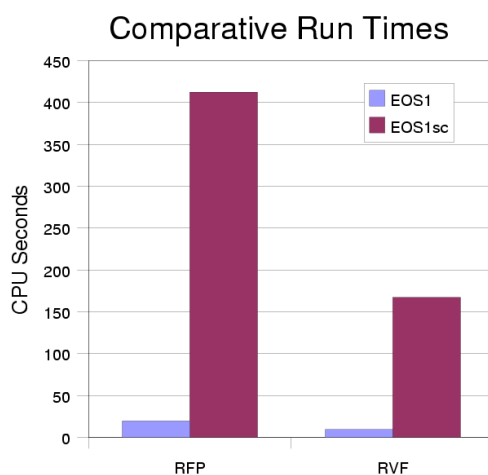


Figure 5: Comparative run times, EOS1 (blue) and *EOS1sc* (magenta). *EOS1sc* runs require 5-10 times more CPU time, since series-based computation of water properties is extremely accurate but time-consuming.

3.2 Supercritical Tests

3.2.1 GEOTHERMAL FIVE-SPOT (RFP)

For familiarity, RFP, the sub-critical EOS1 sample problem treating the “five-spot” injection/production geometry was extended to supercritical conditions. Starting conditions in the reservoir were specified similar to those found at the bottom of well WD-1a at Kakkonda, Japan (Ikeuchi *et al.*, 1998), albeit ignoring the very high salinities encountered at those depths. This test is meant to simulate the conditions that might be encountered in production from a barely supercritical reservoir, e.g. as proposed by Fridleifsson and Albertsson (2000) and modeled by Yano and Ishido (1998). Problem specifications are identical to the RFP problem included in the *TOUGH2* distribution, except that rock initial temperature is set to 400°C, pressure at 22.06 MPa (critical point is located at 373.917 °C, 22.046 MPa, Levelt-Sengers *et al.*, 1983). Fluids at 100 °C are injected at the center of the 5-spot grid, and are withdrawn at an identical rate at the corner of the grid. Non-convergence (using the solver settings given in the distributed RFP file) forced reduction of the pumping rate from 3 kg/sec steam in the subcritical case, to 0.9 kg/sec. Grid refinement was not attempted, but would presumably allow convergence for the higher pumping rate. P-T conditions in the reservoir sweep across the critical point, with the injection point moving rapidly to lower temperatures, then all points moving more slowly upward to lower pressures (Fig. 6). Intermediate points (e.g. element “DA 1”, blue line, Fig. 6) passes through the critical point of pure H₂O, and parallels the two-phase boundary after that. Since the P-T profile between injector and producer (thin black lines, Fig. 6) migrate across the critical point, implied phase transitions are encountered in the grid and are successfully treated by *EOS1sc*.

3.2.2 GENERIC EXTENSIONAL SETTING

A number of detailed thermal models have been made of hypothetical (e.g. Wisian, 2000; Forster and Smith, 1989) and natural (e.g. Becker and Blackwell, 1993) extensional systems, primarily using the U.S. Basin and Range province as the basis for the models. In particular, Wisian (2000) models a system similar to the natural system at Dixie Valley, NV. Comparison

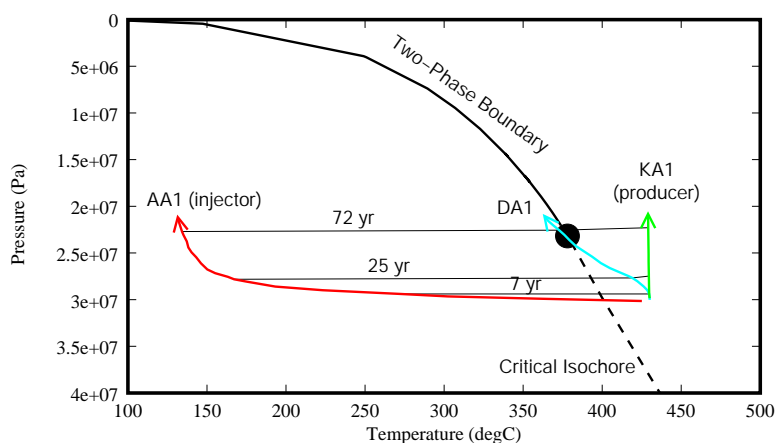


Figure 6: P-T paths for selected wells, supercritical RFP test using *EOS1sc*. Variation of P-T conditions with time at three points along injector-producer line. Points at representative times connected by dashed lines. Injector point migrates rapidly from supercritical initial conditions through critical point to cool liquid conditions. Intermediate point “DA 1” passes directly through critical point, production point “KA1” shows isothermal depressurization.

of temperature-depth profiles made with some of his models (using *TOUGH2* with *EOS1*, see blue line, Fig. 7) shows that modeled temperatures are well below those observed in deep wells in these systems. Wisian’s models extend to 8 km depth in order to avoid boundary effects on fluid flow. At those depths in high heat-flow areas, conditions approach the critical point. To correctly model mass and heat balances in these systems, models must include super-critical conditions even though the produced fluids in such systems never experience such extreme temperatures. A simple experiment with increased (probably excessive) heat input at the base of such a model demonstrates that inclusion of supercritical conditions in the model (using *EOS1sc*, red line, Fig. 7) greatly improves the fit to observed temperature-depth profiles.

4 Summary

A supercritical equation of state for pure H_2O has been developed for use with *TOUGH2*. This module extends the range of *TOUGH2* to beyond typical silicic magma solidus conditions, thereby allowing models of the entirety of magmatic and other high-temperature geothermal systems. This allows the modeler to start from relatively reliable estimates of total mass or energy in the system, rather than having to impose arbitrary boundary conditions based on the limitations of the reservoir simulator. Deep exploration and concerns about sustainable management of geothermal resources require that these deep roots of the system be considered. Preliminary testing of the module demonstrates that it preserves existing accuracy of *TOUGH2* at subcritical conditions, and successfully extends the modeling capabilities to supercritical conditions. Most problematic are systems that contain the critical point, e.g. any system with atmospheric conditions at the top, and supercritical conditions at depth. Difficult solution convergence owing to accurate treatment of fluid property extrema near the critical point requires careful application of *TOUGH2* with *EOS1sc*. Wise choice of matrix solvers, and minimization of steep pressure and temperature gradients in initial conditions generally overcomes these limitations.

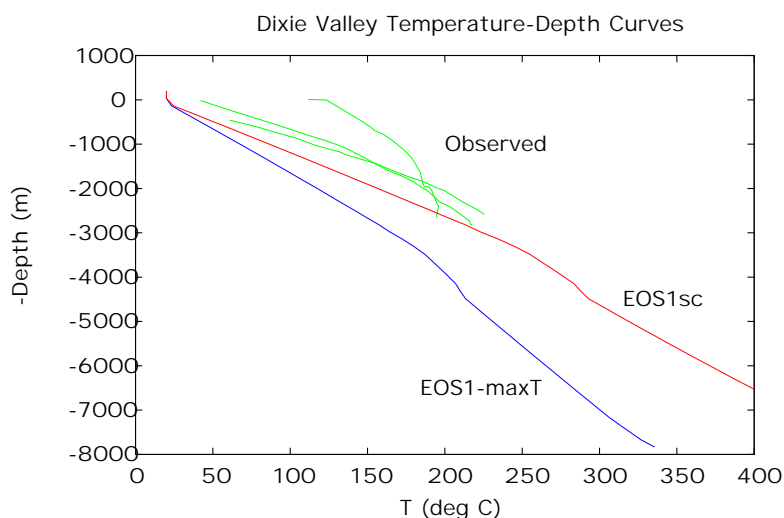


Figure 7: Blue line shows *TOUGH2* model results using EOS1 at maximum allowable temperatures, red line shows results using *EOS1sc* with supercritical conditions at depth. Green lines show observed temperatures at Dixie Valley, NV, after Blackwell *et al.* (2000). Incorporation of supercritical conditions appears to be necessary at base of these basin-scale models in order to match observed T-depth profiles. See Wisian (2000) for details of model construction.

5 Acknowledgments

This research supported by U. S. Dept. of Energy grant DE-FG07-98ID13677 to UTD, with subcontracts to David Blackwell of SMU and Denis Norton, consultant, Stanley ID. Their contributions to the conceptual aspects of this software development have been crucial. James Johnson of LLNL provided the source code for *H2092*. Karsten Pruess provided encouragement in the early stages of this development. Invaluable periodic testing of earlier versions of *EOS1sc* has been carried out by Ken Wisian of SMU.

References

- Becker, D. J., Blackwell, D., 1993. Gravity and hydrothermal modeling of the Roosevelt Hot Springs area, Southwestern Utah. *J. Geophys. Res.* 98, 17787–17800.
- Blackwell, D. D., Golan, B., Benoit, D., 2000. Temperatures in the Dixie Valley, Nevada Geothermal System. *Geotherm. Resour. Council Transact.* 24, 223–28.
- Brikowski, T. H., Norton, D., 1989. Influence of magma chamber geometry on hydrothermal activity at mid-ocean ridges. *Earth Planet. Sci. Lett.* 93, 241–255.
- Forster, C., Smith, L., 1989. The influence of groundwater flow on thermal regimes in mountainous terrain: A model study. *J. Geophys. Res.* 94, 9439–9451.
- Fridleifsson, G. O., Albertsson, A., 2000. Deep geothermal drilling on the Reykjanes Ridge: Opportunity for international collaboration. In: *Proceedings of the World Geothermal Congress 2000*, International Geothermal Organization, pp. F7–5, paper R0882.

- Hayba, D. O., Ingebritsen, S. E., 1994. The computer model HYDROTHERM, a three-dimensional finite-difference model to simulate ground-water flow and heat transport in the temperature range of 0 to 1,200 degrees C. Wri 94-4045, U. S. Geol. Survey, Denver, CO.
- Ikeuchi, K., Doi, N., Skagawa, Y., Kamenosono, H., Uchida, T., 1998. High-temperature measurements in well WD-1a and the thermal structure of the Kakkonda geothermal system, Japan. *Geothermics* 27 (5/6), 591–607.
- International Formulation Committee, 1967. A formulation of the thermodynamic properties of ordinary water substance. IFC Secretariat, Düsseldorf, Germany.
- Johnson, J. W., Norton, D., 1991. Critical phenomena in hydrothermal systems: State thermodynamic, electrostatic, and transport properties of H₂O in the critical region. *Am. J. Sci.* 291, 541–648.
- Johnson, J. W., Oelkers, E. H., Helgeson, H. C., 1992. SUPCRT92; a software package for calculating the standard molal thermodynamic properties of minerals, gases, aqueous species, and reactions from 1 to 5000 bar and to 1000 degrees C. *Computers & Geosciences* 18 (7), 899–947.
- Levelt-Sengers, J. M. H., Kamgar-Parsi, B., Balfour, F. W., Sengers, J. V., 1983. Thermodynamic properties of steam in the critical region. *J. Phys. Chem. Ref. Data* 5 (1), 1–51.
- Muraoka, H., Yasukawa, K., Kimbara, K., 2000. Current state of development of deep geothermal resources in the world and implications to the future. In: Iglesias, E., Blackwell, D., Hunt, T., Lund, J., Tmanyu, S. (eds.), *Proceedings of the World Geothermal Congress 2000*, International Geothermal Association, pp. 1479–1484.
- Norton, D. L., Hulen, J. B., 2000. Geologic Analysis and Thermal-History Modeling of The Geysers Magmatic-Hydrothermal System. *Geothermics* p. 12, in press.
- Pruess, K., Oldenburg, C., Moridis, G., 1999. TOUGH2 User's Guide, Version 2.0. Report LBNL-43134, Lawrence Berkeley Nat. Lab, Berkeley, CA.
- Vinsome, K., 1990. TETRAD User Manual. Dyad Engineering, Calgary, Alberta, Canada.
- Whitney, J. A., 1975. The effects of pressure, temperature and $\chi_{\text{H}_2\text{O}}$ on phase assemblage in four synthetic rock compositions. *J. Geol.* 83, 1–31.
- Wisian, K. W., 2000. Insights into Extensional Geothermal Systems from Numerical Modeling. *Geotherm. Resour. Council Transact.* pp. 281–286.
- Yano, Y., Ishido, T., 1998. Numerical Investigation of Production Behavior of Deep Geothermal Reservoirs at Super-Critical Conditions. *Geothermics* 27 (5/6), 705–721.